OPTOELECTRONICS AND ADVANCED MATERIALS – RAPID COMMUNICATIONS Vol. 3, No. 11, November 2009, p. 1195 - 1199

Magnetic and structural investigations of nanocrystalline nickel ferrite $NiFe_2O_4$

A. ADAM, Z. ALI*, E. ABDELTWAB, Y. ABBAS[a]
Physics Department, Faculty of Science (Girls Branch), Al-Asher University, Cairo, Egypt
[a]*Physics Department, Faculty of Science, Suez canal University, Ismailia, Egypt*

Nickel ferrite is an important high frequency magnetic material due to its ultrahigh resistivity. Nanoparticles of $NiFe_2O_4$ ferrite have been synthesized by the chemical co-precipitation of the amorphous metal hydroxides (under controlled pH values) . The prepared powder have been sintered at 850°C. Room temperature X-ray measurements of the prepared sample of $NiFe_2O_4$ reveal the production of single cubic phase with average particle size of about 53 nm. The lattice parameters, the oxygen position and the cation distribution have been determined by using Rietveld analysis. The particle morphology was studied by scanning electron microscopy (SEM) and transmission electron microscopy (TEM). The different morphologies, sizes, material properties and magnetic behavior between these spinels were analyzed and discussed. The Fourier transform infrared (FT-IR) spectral study on the nanocrystalline $NiFe_2O_4$ ferrite phase was recorded between 400 and 1000 cm^{-1}. Two fundamental absorption bands appear at 608 cm^{-1} and 424 cm^{-1} characteristics of metal vibrations. The results of the Vibrating Sample Magnetometer (VSM) indicate the correlation between the magnetic properties and the nanocrystallinity of the investigated nickel ferrite.

(Received June 25, 2009; accepted October 29, 2009)

Keywords: Nanoparticals, Ferrites, Magnetization

1. Introduction

Spinels of general formula AB_2O_4 are known to be technologically important materials because of their tailorable properties to meet stringent requirements in various applications [1, 2]. Especially ferrites belonging to this class of materials are gaining prominence owing to their efficacious properties such as high thermodynamic stability, high electrical conductivity, and high corrosion resistance, making them suitable in metallurgical field and other high temperature areas. Nickel ferrite and its derivatives have been tried as inert anodes for electrometallurgical applications particularly for the production of aluminum using Hall Heroult process [3, 4].

Nanosize spinel ferrite particles have attracted considerable attention and continued efforts to investigate them for their technological importance to the microwave industries, high speed digital tap or disk recording, repulsive suspension for use in levitated railway systems, ferrofluids, catalysis and magnetic refrigeration systems [5-7]. The conventional way of preparing the ferrite is by solid-state reaction, which involves the mixing of oxides with intermittent grinding followed by high temperature sintering between 1300 and 1700 °C. Though the process remains simple it has several drawbacks such as high reaction temperature, larger particle size, limited degree of homogeneity, and low sinterability. On the other hand, the wet chemical processes such as sol gel, co-precipitation, citrate-gel and combustion synthesis method yield sub-micron sized particles with good homogeneity, high sinterability, and good control of stoichiometry [8]. Further the combustion synthetic route is preferred, because of its potential advantages such as low processing time, low external energy consumption, and self-sustaining.

Present studies on $NiFe_2O_4$ system is focused on the production of the nanosized materials at very low temperatures so that the nanosized material produced can be sintered at relatively lower temperatures, compared to the high temperatures required for materials synthesized by the conventional ceramic method [9,10].

In the present work the nanosized $NiFe_2O_4$ has been prepared by co-precipitation synthetic method. Several complementary experimental techniques have been used to investigate the structure and magnetic properties: X-ray diffraction, electron microscope, FT infrared spectroscopy and magnetic measurements. Several computer programs have been used for the analysis of the experimental results.

2. Experimental procedure

Nanocrystalline Ni ferrite particles were synthesized by the chemical co- precipitation method. The starting materials are high-purity $NiSO_46(H_2O)$ and $FeSO_47(H_2O)$. According to the formula of $NiFe_2O_4$ each starting material was weighted, all added into 500 ml de-ionized water with concentration of 0.25 M, and stirring to complete dissolution. The NaOH solution is prepared by dissolving NaOH into 500 ml de-ionized water with concentration of 1M. These two solutions mentioned above are mixed together by stirring, heated to the reaction temperature between 90 and 200 ° C, and aerated

uniformly by pumping air through porous glass to promote an oxidization reaction for 6 h. During oxidation, a small amount of NaOH solution was continuously added to keep the pH value at 12. After 6 h of reaction, the precipitated particles are washed and filtered six times then dried at 60 ^{o}C. After drying, the co-precipitated ferrite particles were sintered at 850 ^{o}C for 2 h.

The crystalline structure of the precipitated particles X-ray diffraction measurements were performed by means of an X-ray diffractometer (Philips X' pert MPP) with Cukα (λ=1.54056 Å) radiation. X-ray powder diffraction data were obtained in a 2.0 scanning range from 10 to 80 with a step size of 0.03 (2θ) with 8.0 sec counting time at each step.

Morphology and microstructure of the powder were studied on a JEOL, 6400 scanning electron microscope (SEM), and the Transmission electron microscopic (TEM) images were obtained on a JEOL-1230 microscope with an accelerating voltage of 100keV. The Fourier Transform Infrared Spectroscopy (FT-IR) spectrum was recorded as (KBr) discs in the range 400–1000 cm^{-1} using (FT-IR–Beckman-4250) spectrophotometer. The magnetic measurements of the prepared powder have been determined at room temperature using LDJ (Model 9600) vibrating sample magnetometer (VSM) in a maximum external field of 16 kOe.

3. Results and discussion

3.1 X-ray diffraction

X-ray diffraction pattern of the - synthesized $NiFe_2O_4$ is presented in Fig. 1. It is observed that the peaks corresponding to the planes (3 1 1), (4 4 0), (2 2 0), confirming the phase formation of pure $NiFe_2O_4$ with a well-defined spinel structure without any impurity phase and coinciding with the (ICDD PDF #74-2081). The variation of the Miller indices (h, k, and l) with the spacing (d) for Ni Fe_2 O_4 prepared sample was given in table (1). A fitting refinement procedure performed using FULLPROF Rietveld software [11, 12]. Table 2 shows the refinement results for nanocrystalline N iFe_2O_4 .The model and experimental data are in good agreement confirming the cubic spinel structure corresponding to the *Fd3m* space group. The Rietveld plot of the refinement is given in Fig. 2. In this figure the observed intensity data, y is plotted in the upper field as points. The calculated patterns are shown in the same field as a solid- line curve. The difference, observed minus calculated, is shown in the lower field. The short vertical bars in the middle field indicate the positions of possible Bragg reflections. Fig. 3 Zoom out of a part of the pattern of the profile fitting for nanocrystalline $NiFe_2O_4$ to represent the agreement between the observed and calculated data. The fitting parameters values of the sample indicate that the profile was fitted successfully. The lattice parameter a, and the oxygen parameter U were calculated and found to be *a* = 0.8335 nm, and U = 0. 2549 respectively.

It is well known that the magnetic properties of spinel ferrites depend on the summation of magnetic moments at the A and B sites [13]. It has been also experimentally verified that the distribution of cations among the lattice sites depends on material's preparation. Profile fitting by Rietveld analysis is the most general method to determine the site occupation factors.

The cation distribution on A- site and B- site for nanosize $NiFe_2O_4$ prepared sample is found to be:

$$\text{(A site)} \qquad \text{[B site]}$$

$$(Ni_{0.07}\ Fe_{0.93})\ [Ni_{0.93}\ Fe_{1.07}]$$

The refinement results showed that the nanocrystalline ferrite phase is partially an inverse spinel. The formation of mixed spinel instead of inverse spinel may result from that during the formation of spinel ferrite the occupancy of Fe^{3+} cation on (A) site decreases. At the same time, the occupancy of Ni^{2+} cation on [B] site decreases and then increases on (A) site. This occurs when the random distribution of cations among the (A) and [B] sites inside the spinel matrix exist.

The inter atomic distances between the cations on the tetrahedral (A) and octahedral (B) sites are found to be as follows:

$$R_A - R_A = (\sqrt{3}/4)\,a = 3.6091 \quad (1)$$

$$R_A - R_B = (\sqrt{11}/4)\,a = 3.6933 \quad (2)$$

$$R_B - R_B = (\sqrt{2}/4)\,a = 2.9468 \quad (3)$$

$$R_A - O_A = a\sqrt{3}\,(\delta + 1/8) = 1.8733 \quad (4)$$

$$R_B - O_B = a\,[1/16 - \delta/2 + 3\delta^2]^{1/2} = 2.0435 \quad (5)$$

where δ is deviation from oxygen parameter (U) , R_A and R_B refer to the cations at the center of the tetrahedral (A) and octahedral (B) Sites respectively, while O_A and O_B refer to the center of an oxygen anion, related to the tetrahedral (A) and octahedral (B) configuration respectively. These parameters are necessary to give full description of the crystallographic structure, and are of interesting in connection with the magnetic properties.

Magnetic properties of ferrites have been explained by Neel [14], who postulated that magnetic moments of ferrites are a sum of magnetic moments of individual sublattice M_A and M_B. The magnetic moments on the A and B sites to be antiparallel oriented whereas those on the B-sites are parallel to each other.

In the present work it is found that $M_A = 4.79\ \mu_B$, $M_B = 7.21\ \mu_B$ and the net magnetic moment μ / molecule $= |M_A - M_B| = 2.42\ \mu_B$.

Table 1. the variation of the Miller indices (h, k, and l) with the spacing (d) for Ni Fe_2O_4 co- precipitation prepared sample.

h k l	d(Å)	$\sqrt{h^2+k^2+l^2}$	$1/d(Å)^{-1}$
1 1 1	4.8123 (9)	1.7320	0.2077
2 2 0	2.9469(6)	2.8284	0.3393
3 1 1	2.5131(3)	3.3166	0.3979
2 2 2	2.4061(9)	3.4641	0.4155
4 0 0	2.0838(2)	4.0000	0.4798
3 3 1	1.9122(5)	4.3588	0.5229
4 2 2	1.7014(3)	4.8989	0.5877
3 3 3	1.6041(7)	5.1961	0.6233
4 4 0	1.4734(8)	5.6568	0.6786
5 3 1	1.4089(2)	5.9160	0.7097

Table 2. Refinement results for $NiFe_2O_4$ co-precipitation prepared sample.

h k l	2Θ	I_{obs}	I_{calc}	I_o-I_c
1 1 1	18.467	135	160	25
2 2 0	30.381	417	473	56
3 1 1	35.788	1585	1514	71
2 2 2	37.341	83	89	6
4 0 0	43.388	346	307	39
3 3 1	47.508	9	8	1
4 2 2	53.837	163	134	29
3 3 3	57.395	489	405	84
4 4 0	63.210	584	549	35
5 3 1	66.470	14	9	5

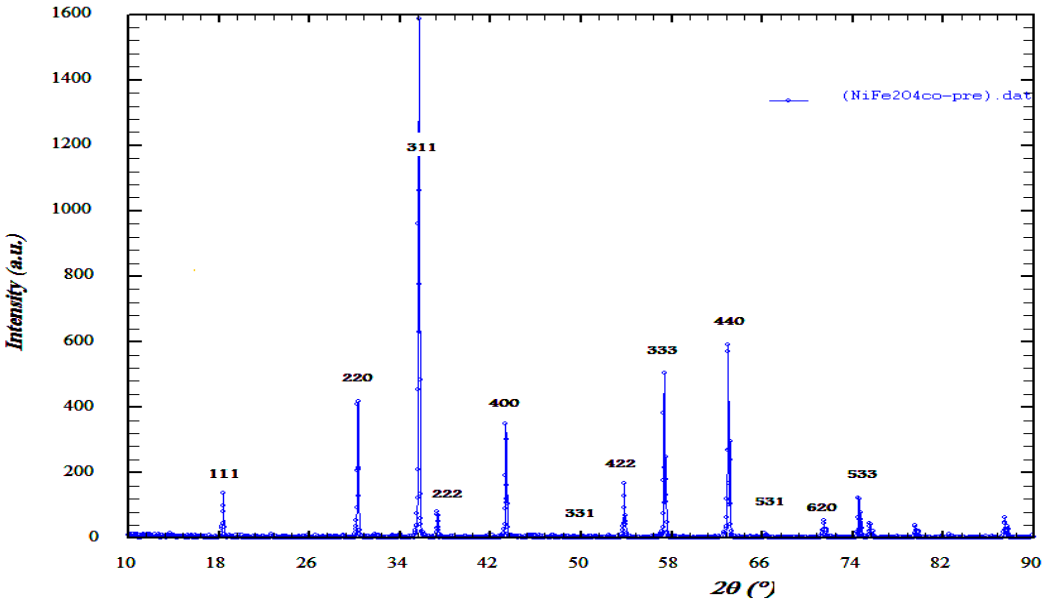

Fig. 1. X-ray diffraction pattern for Ni Fe_2O_4 prepared sample.

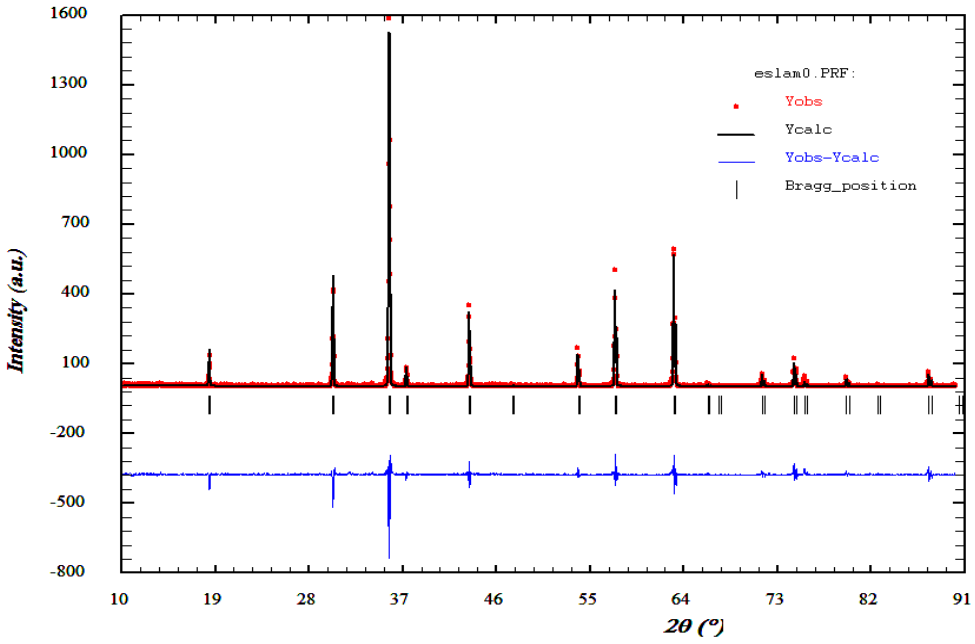

Fig. 2. The profile fitting for the Ni Fe_2O_4 prepared sample.

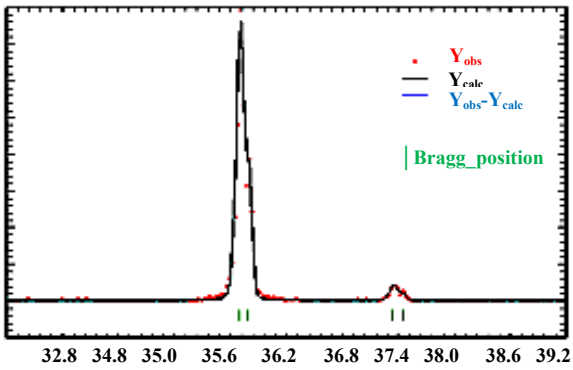

Fig. 3. Zoom out of a part of the pattern of the profile fitting for $NiFe_2O_4$ prepared sample .

3.2 Microstructure analysis

Rietveld analysis [15] has been adopted in the present study to determine the microstructure parameters of nanocrystalline $NiFe_2O_4$. The analysis aims to characterize the materials in terms of microstructure parameters such as crystallite size and root mean square (r.m.s) lattice strain. Average crystallite size and lattice strain calculated from Win-Fit programme are found to be 53 nm and 0.047%, respectively.

3.2.1 Scanning electron microscope (SEM)

The microstructure and Surface morphology was observed with a scanning electron microscopy (SEM). SEM representative micrograph for the nanocrystalline $NiFe_2O_4$ ferrite prepared by co-precipitation method shown in Fig. 4. The surface morphology of the sample as seen from the SEM consists of well-crystallized grains, with relatively homogeneous grain distribution, with an average grain size varying from 1 to 3μm.

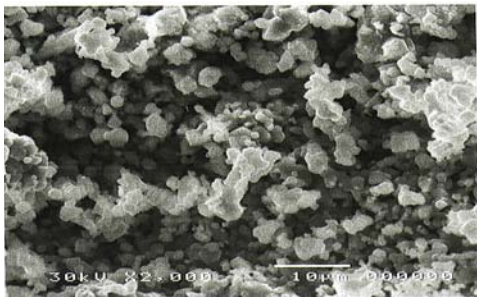

Fig. 4. SEM image for the nanocrystalline $NiFe_2O_4$.

3.2.2 Electron microscope (TEM)

TEM delivers very valuable information concerning the grain size and appearing phases, unfortunately the sample preparation is not simple. Microstructure of the nanocrystalline ferrite $NiFe_2O_4$ has been characterized by TEM. TEM micrograph for Ni Fe_2O_4 shown in Fig. 5 reveals that the grains of the sample are spherical in shape and average size of the particles (≈ 60 nm) is quite closer to the X-ray crystallite size. The shape of Ni Fe_2O_4 precipitated particles becomes regular and the distribution of particle size is uniform. However, some of the particles are quite bigger due to agglomeration of small grains and variation in density of grains clearly corroborates the findings. The non-uniform particles size distribution should attribute to a non-uniform ingredient mixture and a non-uniform grain distribution of powder.

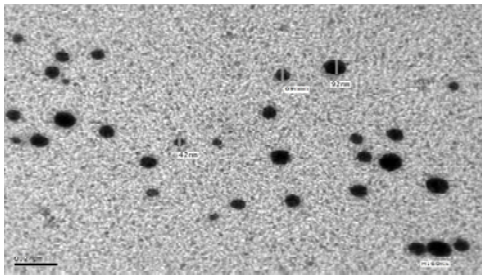

Fig. 5. Transmission electron microscope (TEM) for Ni Fe_2O_4 co-precipitation prepared sample.

3.3 Fourier transformation infrared (FT-IR)

The IR spectral study on the nanocrystalline $NiFe_2O_4$ ferrite phase was recorded between 400 and 1000 $cm^{-1}$and is shown in Fig. 6.

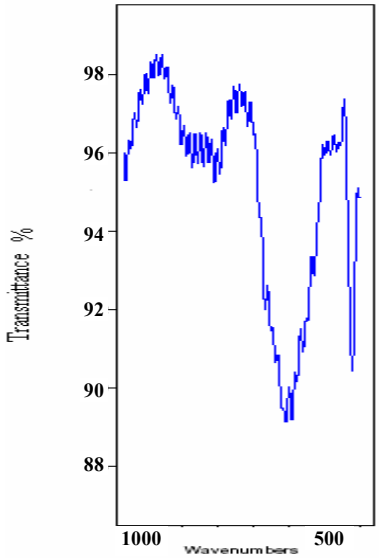

Fig. 6. FT-IR spectrum of nanosize Ni Fe $_2O_4$.

The spectrum elucidates the position of the ions in the crystal structure and their vibration modes, which represents the various ordering positions on the structural properties of the synthesized compound. The absorption bands for the synthesized ferrite are in the expected range. The spectrum shows two absorption bands around 608, and 424cm^{-1}. According to Waldron [16], the high frequency band υ_1 around 608cm^{-1} is attributed to that of tetrahedral complexes. The band υ_2 around 424cm^{-1} corresponding to octahedral complexes. The variation in

the band positions is due to the difference in the Fe^{3+}– O^{2-} distances for the octahedral and tetrahedral complexes [17]

3.4 Magnetic properties

The magnetization curve of the nickel ferrite nano-octahedrons measured at room temperature is shown in Fig. 7. The sample presented excellent softmagnetic property with coercivity (Hc) less than 30 Oe, while at 10K the coercivity increased to 268 Oe. The saturation magnetization (Ms) of the sample was 49.6 emu/g, close to the bulk value of nickel ferrite. It is well known that for magnetic particles the size has significant influence on their magnetic properties. For relatively larger particles, magnetic domains are formed to reduce the static magnetic energy. The number of domains diminishes with decreasing particle size. The particles turn into single domain ones with their size under a critical radius (for nickel ferrite, this parameter is about 100nm [18]), resulting in the increasing coercive force due to vanishing of the magnetization caused by the movement of domain walls. It was earlier reported by Morrish et al. [19] that at room temperature the nickel ferrite nanoparticles, with irregular shapes and sizes from 60 to 100nm, exhibited less saturation magnetization (37.6 emu/g) and much larger coercivity (500 Oe) compared to the values of their bulk counterpart. Although the size distribution of particles in our experiment is in the similar region to that of literature [20], the coercive force is much lower .

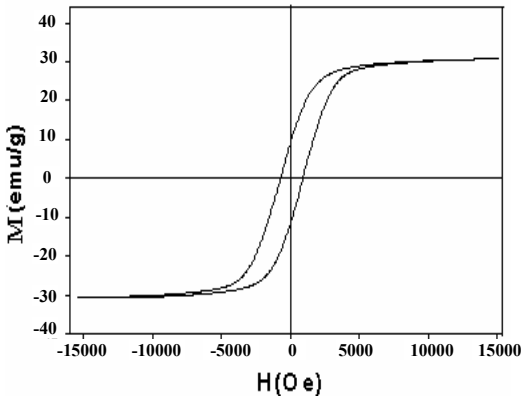

Fig. 7. Plots of magnetization vs. applied field for Ni Fe $_2$ O_4 prepared sample.

4. Conclusions

1-The wet chemical co-precipitation method has been successfully used for the preparation of Nickel spinel ferrite with nanosize particles, provide the higher degree of homogenization of reactant and lower temperature is sufficient for the reaction to occur, high sinterability, and good control of stoichiometry.

2-The refinement results showed that the nanocrystalline ferrite phase is partially an inverse spinel. The formation of mixed spinel instead of inverse spinel may result from that during the formation of spinel ferrite the occupancy of Fe^{3+} cation on (A) site decreases. At the same time, the occupancy of Ni^{2+} cation on [B] site decreases and then increases on (A) site. This occurs when the random distribution of cations among the (A) and [B] sites inside the spinel matrix.

3-For characterizing nanocrystalline magnetic materials, a line profile analysis is the most common used method. However, the problem is that the line profile is also influenced by local stresses.

4-The surface morphology of the sample as seen from the SEM consists of well-crystallized grains, with relatively homogeneous grain distribution.TEM micrograph reveals that the grains of sample are spherical in shape and average size of the particles is quite closer to the X-ray crystallite size.

5-The nanocrystalline Ni Fe_2O_4 shows absorption bands around 608, and 424 cm^{-1}. The high frequency band ν_1 around 608 cm^{-1} is attributed to tetrahedral complexes and the band υ_2 around 424cm^{-1} corresponding to octahedral complexes.

6-The magnetic properties of the sample clearly depend on the size of the nanocrystallites. The magnetic properties of a spinel ferrite are strongly dependent on the distribution of the different cations among (A) and [B] sites and on the material's preparation.

References

[1] L. Sathyanarayana, K. Madusudhan Reddy, S. V. Manorama, Mater. Chem. Phys. **82**, 21 (2003).
[2] R. Alcantra, M. Jaraba, P. Lavela, J. L. Tirado, J. C. Jumas, J. Oliver, Electrochem. Commun. **5**, 16 (2003).
[3] E. Olsen, J. Thonstad, J. Appl. Electrochem. **29**, 293 (1999).
[4] L. John Berchmans, R. Kalai Selvan, C. O. Augustin, Mater. Lett. **58**, 1928 (2004).
[5] T. Pannaparayil, R. Marande, S. Komarneni, S. G. Sankar, J. Appl. Phys. **64**, 5641 (1988).
[6] A. Goldman In: Levenson (ed) Electronic Ceramics. Marcel Dekker, New York, 170, 1988.
[7] J. L. Dormann, D. Fiorani, Magnetic Properties of Fine Particles. North-Holland, Amsterdam, 1992.
[8] D. Siegel, J. Mater. Chem. **7**, 1297 (1997).
[9] Z. Zhong, Q. Li, Y. Zhang, H. Zhong, M. Cheng, Yang Zhang Powder Technology **155**, 193 (2005).
[10] I. Stambolovaa, A. Tonevab, V. Blaskova, D. Radeva, Ya. Tsvetanovab, S. Vassilevc, P. Pesheva, J. of Alloys and Compounds **391**, L1 (2005).
[11] H. M. Rietveld, Acta Crystallogr. **22**, 151 (1967).
[12] H. M. Rietveld, J. Appl. Crystallogr. **2**, 65 (1969).
[13] S. K. Pradhan, S. Bidb, M. Gateshki, V. Petkov, Materials Chemistry and Physics **93**, 224 (2005).
[14] L. Neel, Ann. Phys. Paris **3**, 137 (1948).
[15] L. Lutterotti, MAUDWEB, Version 1.9992, 2004; http://www.ing. unitn.it/luttero/maud.
[16] R. D. Waldron, Phys. Rev. **99**, 1727 (1955).
[17] A. K. Ghatage, S. C. Choudhari, S. A. Patil, J. Mater. Sci. Lett. **15**, 1548 (1996).
[18] I. S. Jacobs, C. P. Bean, Phys. Rev. **100**, 1060 (1955).
[19] A. H. Morrish, K. Haneda, J. Appl. Phys. **52**(3), 2496 (1981).
[20] A. S. Albuquerque, J. D. Ardisson, W. A. A. Macedo, J. L. Lopez, R. Paniago, A. I. C. Persiano, J. Magn. Magn. Mater. **226-230**, 1379 (2001).

*Corresponding author: zeinab_ali@maktoob.com